

## SUPPLEMENTARY MATERIALS



**Figure S1.** Sampling points and corresponding samples (powders and fragments) observed under stereomicroscope.

**Table S1.** For each XRF point of analysis, elements detected and detail of the analyzed surface. Key to notation: **bold** = major, normal = minor, *italic* = trace, (*italic*) = very trace. E: eastern; W: western; f: front; b: back; \*: poorly reliable results due to measurement point difficult to probe.

Point	Eagle	Description	Elements	Detail of point of analysis
01	E, b	Red paint on feather	<b>Cu, Ca, Au, Pb, Fe, Hg, K, (Mn), Sn, (Sb)</b>	
02	E, b	Feather, right wing	<b>Cu, Ca, Au, Pb, Fe, Sn, (Sb), (K)</b>	
03	E, b	Bale of cloth	<b>Cu, Ca, Fe, Pb, Ag, As, K, Mn, Sn, (Sb)</b>	
04	E, b	Lanyard of the bale of cloth	<b>Cu, Ca, Au, Pb, Fe, Sn, Sb, Mn, K, (Ag)</b>	
05	E, b	Dark patina on bale of cloth	<b>Cu, Ca, Pb, Sn, Fe, K, Ag, (As), (Sb)</b>	

06	E, b	Feather on the tail	<b>Cu, Ca, Au, Fe, Pb, Sn, K, Mn, Si, (Sb)</b>	
07F	E, b	Red paint on feather	<b>Cu, Hg, Au, Pb, Sn, Fe, (Sb)</b>	
08F	E, b	Feather, right wing	<b>Cu, Au, Sn, Pb, Fe, Sb</b>	
09F	E, b	Feather, right wing	<b>Cu, Au, Sn, Pb, Fe, Sb</b>	
10	E, b	Feather, right wing	<b>Cu, Ca, Au, Fe, Pb, Sn, Sb, K, Mn</b>	
11	W, f	Beak	<b>Cu, Ca, Au, Sn, Pb, Fe, Sb, K, (Mn)</b>	

12	W, f	Claw	<b>Cu, Ca, Hg, Fe, K, Pb, Sn, Sb, Mn</b>	
13	W, f	Claw	<b>Cu, Ca, Hg, Sn, Pb, Fe, Si, Cl, K, Mn, (Sb)</b>	
14	W, f	Beak	<b>Cu, Ca, Au, Sn, Pb, Fe, K, (Mn), (Sb)</b>	
15	W, f	Claw	<b>Cu, Ca, Sn, Pb, Fe, Hg, Si, Cl, K, Mn, (Sb)</b>	
16	W, f	Right paw	<b>Cu, Ca, Sn, Pb, Fe, Si, As, Cl, K, Mn, (Sb)</b>	
17	W, f	Bale of cloth	<b>Cu, Ca, Fe, Pb, Ag, As, K, Mn, Sn, (Sb)</b>	

---

18	W, f	Lanyard on the bale of cloth	<b>Cu, Ca, Au, Fe, Pb, Sn, K, (Mn), (Sb)</b>	
19	W, f	Feather, left wing	<b>Cu, Ca, Au, Sn, Pb, Fe, K, Mn, (Sb)</b>	
20	E, f	Beak	<b>Cu, Ca, Au, Sn, Pb, Fe, K, (Mn), (Sb)</b>	
21	E, f	Claw	<b>Cu, Ca, Sn, Pb, Fe, K, (Mn), (Sb)</b>	
22	E, f	Claw	<b>Cu, Ca, Sn, Pb, Fe, K, (Mn), (Sb)</b>	
23	E, f	Left paw	<b>Cu, Ca, Sn, Pb, Fe, K, (As), (Mn), (Sb)</b>	

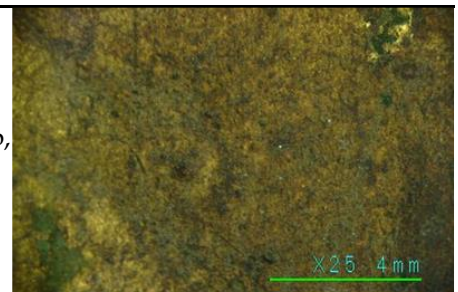
---

24

E, f

Feather, right wing

**Cu, Ca, Au, Sn, Pb,  
Fe, K, (Mn), (Sb)**



25

E, f

Feather on neck

**Cu, Ca, Au, Sn, Pb,  
Fe, (K), (Mn), (Sb)**



26\*

E, f

Inside bale of cloth

**Cu, Fe, Pb, Ca, Sn**



27\*

E, f

Inside bale of cloth

**Cu, Fe, Ca, Pb, Sn,  
(Mn)**



28

E, f

Left paw

**Cu, Ca, Sn, Pb, Fe,  
K, Mn, (Sb)**



29

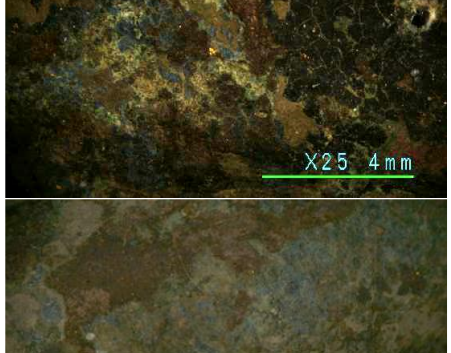
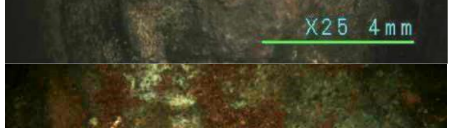
E, f

Bale of cloth

**Cu, Ca, Fe, Pb, Sn,  
Ag, As, K, Mn, (Sb)**

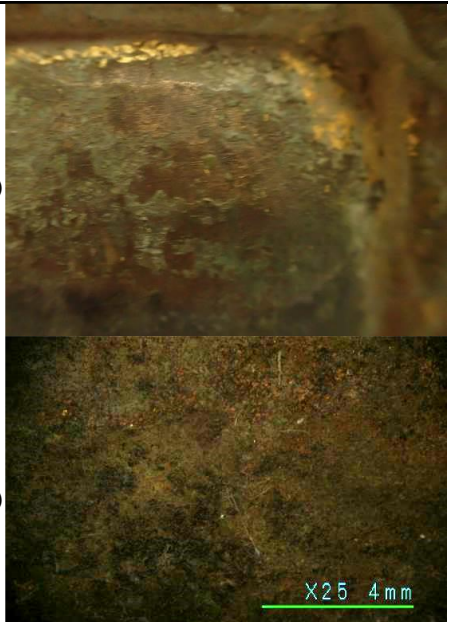


---

30	E, f	Eye	<b>Cu, Ca, Fe, Au, Pb, Sn, (K), (Sb)</b>	
31	E, f	Claw	<b>Cu, Ca, Sn, Pb, Fe, As, K, Si, (Mn), (Sb)</b>	 X25 4 mm
32	E, f	Left paw	<b>Cu, Ca, Sn, Pb, Fe, K, (Mn), (Sb)</b>	 X25 4 mm
33	W, f	Right paw	<b>Cu, Ca, Sn, Pb, Fe, (Sb)</b>	 X25 4 mm
34	W, f	Claw	<b>Cu, Ca, Sn, Pb, Fe, Hg, As, K, Si, (Mn), (Sb)</b>	 X25 4 mm
35	W, f	Eye	<b>Cu, Ca, Fe, Au, Pb, Sn, (K), (Hg), (Mn), (Sb)</b>	 X25 4 mm

---

---

36	W, b	Bale of cloth	<b>Cu, Ca, Fe, Pb, Sn, Ag, (As), (Mn), (Sb)</b>	
37	W, b	Bale of cloth	<b>Cu, Ca, Fe, Pb, Sn, Ag, (As), (Mn), (Sb)</b>	
38	W, b	Bale of cloth	<b>Cu, Ca, Fe, Pb, Sn, Ag, (As), (Mn), (Sb)</b>	n.a.
39	W, b	Bale of cloth	<b>Cu, Ca, Fe, Pb, Sn, Ag, Mn, (As), (Sb)</b>	n.a.
40F	W, b	Bale of cloth, see 36	<b>Cu, Pb, Sn, Sb, Ag, Ca, Fe, (Mn)</b>	n.a.
41F	W, b	Bale of cloth, see 37	<b>Cu, Pb, Sn, Sb, Ag, Ca, Fe, (Mn)</b>	n.a.
42F	W, f	Claw, see 34	<b>Cu, Sn, Pb, Fe, Hg, Ca, (Sb)</b>	n.a.
43F	E, f	Claw, see 31	<b>Cu, Sn, Pb, Fe, Ca, (Ag), (Sb)</b>	n.a.
44F	E, f	Left paw, see 28	<b>Cu, Sn, Pb, Fe, Ca, (Sb)</b>	n.a.
45F	E, f	Claw, see 31	<b>Cu, Sn, Pb, Fe, Ca, Sb, (Ag)</b>	n.a.
46F	E, f	Claw, see 31	<b>Cu, Sn, Pb, Fe, Ca, Sb, (Ag)</b>	n.a.

---

47F	W, f	Claw	<b>Cu, Sn, Pb, Hg, Fe, Ca, Sb, Ag</b>	n.a.
48F	W, f	Eye, see 35	<b>Cu, Au, Pb, Sn, Fe, (Sb)</b>	n.a.
49F	E, f	Eye, see 30	<b>Cu, Au, Pb, Sn, Fe, (Sb)</b>	n.a.
50F	W, f	Claw, see 34	<b>Cu, Au, Pb, Sn, Hg, Fe, Sb, (Ag)</b>	n.a.

**Table S2.** Main vibration bands detected in the samples taken from the eagles, with their assignments.

Compound	Vibration band (cm <sup>-1</sup> )	Assignment	Refs.
Gypsum	3512, 3400 1133	v(OH) v <sub>3</sub> (SO <sub>4</sub> <sup>2-</sup> )	[36]
Calcium oxalate	1644, 1621 1320	v <sub>as</sub> (C=O) overlapping δ(HOH) v <sub>s</sub> (C-O)	[37,38]
Atacamite	3447, 3350 987-846	v(OH) OH deformation	[39]
Moolooite	1367, 1322 828	v <sub>s</sub> (C-O) + δ(O-C=O) δ(O-C=O) + v(Cu-O)	[38,40]
Lipid substance	2927, 2855 1716 3412	v <sub>as</sub> (CH <sub>3</sub> ), v <sub>s</sub> (CH <sub>2</sub> ) v(C=O) v(OH)	[41]
Azurite	1464, 1403 951	v <sub>3</sub> (CO <sub>3</sub> <sup>2-</sup> ) δ(O-H) out-of-plane bending	[42]
Metal carboxylate	2928, 2858 1590-1400 3400	v <sub>as</sub> (CH <sub>3</sub> ), v <sub>s</sub> (CH <sub>2</sub> ) v <sub>a</sub> (COO <sup>-</sup> ), v <sub>a</sub> (COO <sup>-</sup> ) v (N-H)	[43-45]
Proteinaceous substance	1644 1536	v (C = O) (amide I) δ(NH) + v(CN) (amide II)	[46, 47]
Calcium carbonate	1412	v <sub>3</sub> (CO <sub>3</sub> <sup>2-</sup> )	[47]
Silicate	1095	v <sub>as</sub> (Si-O-Si)	[48]

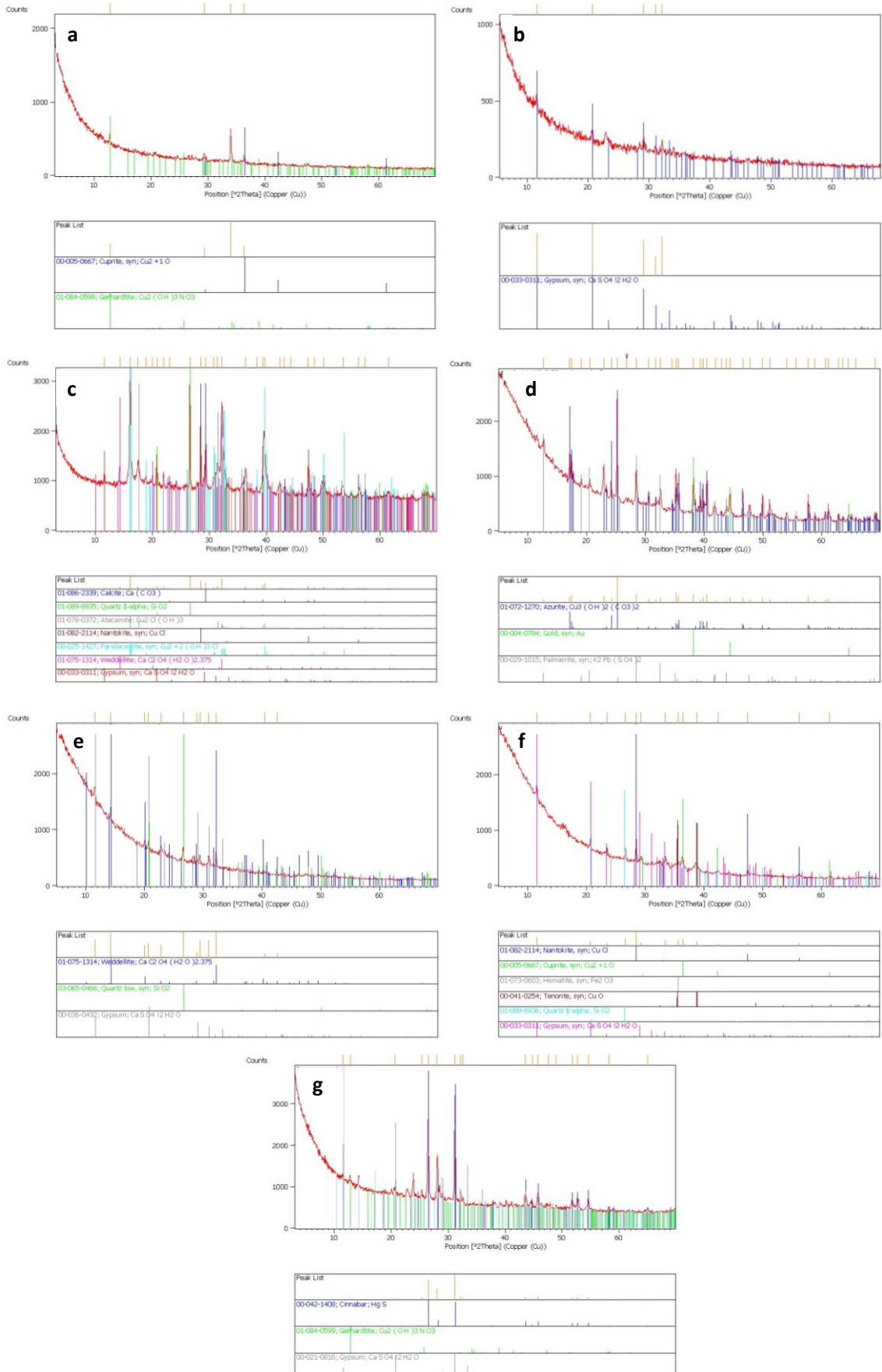


**Figure S2.** XRPD pattern of micro-samples. **(a)** Sample 3; **(b)** Sample 4; **(c)** Sample 6; **(d)** Sample 11; **(e)** Sample 12; **(f)** sample 13; **(g)** Sample 14.

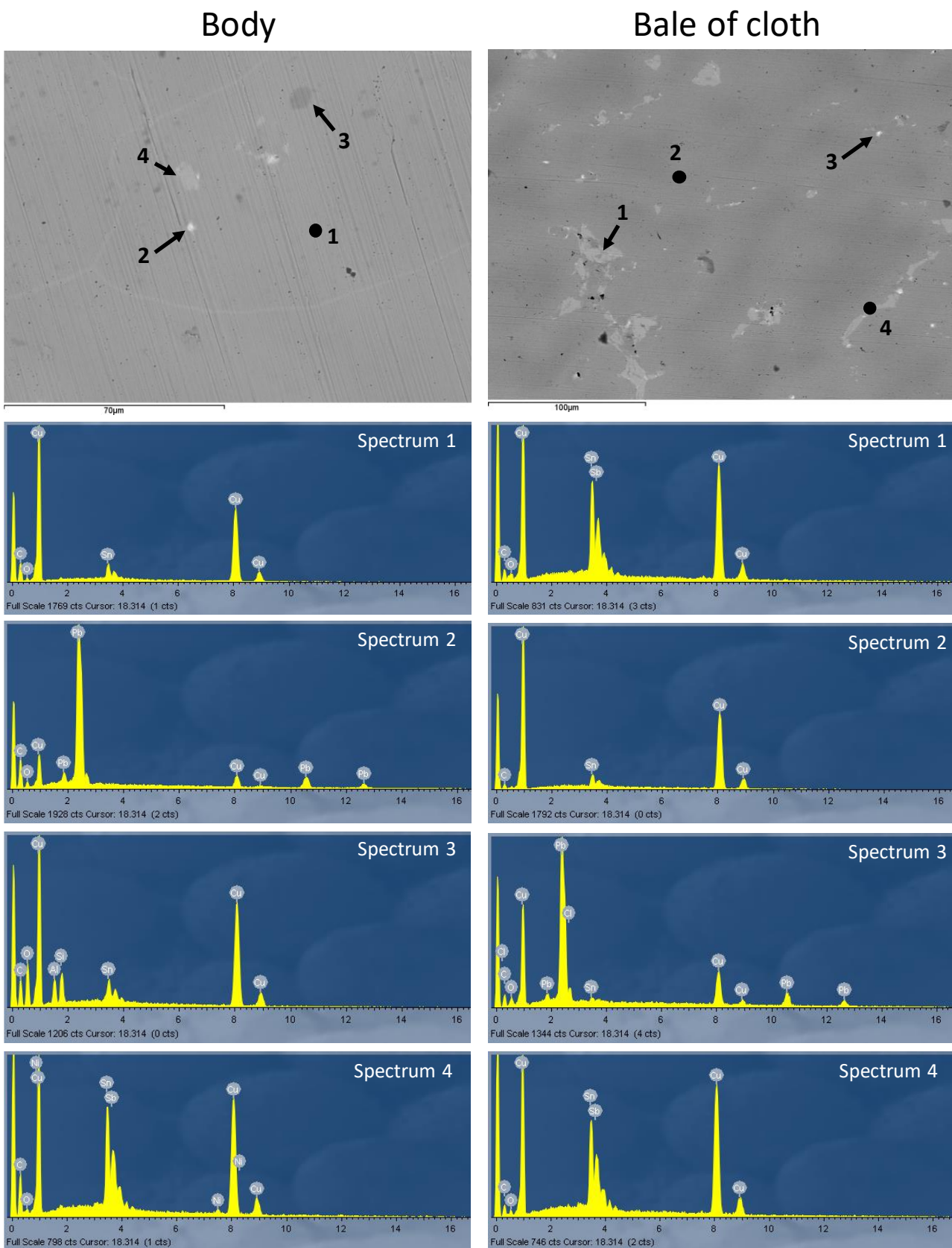


**Figure S3.** SEM-EDS analysis of the alloy of samples 01 (body) and 02 (bale of cloth) from the Western eagle.

## References in Supplementary Materials

36. La Russa, M.F.; Ruffolo, S.A.; Barone, G.; Crisci, G.M.; Mazzoleni, P.; Pezzino, A. The use of FTIR and micro-FTIR spectroscopy: an example of application to Cultural Heritage. *Int J Spectr* 2009.
37. Monico, L.; Rosi, F.; Miliani, C.; Daveri, A.; Brunetti, B.G. Non invasive identification of metal-oxalate complexes on polychrome artwork surfaces by reflection mid-infrared spectroscopy. *Spectrochim Acta Part A: Mol Biomol Spectrosc* 2013, 116:270–280.
38. Frost, R.L. Raman spectroscopy of natural oxalates. *Anal Chim Acta* 2004, 517:207–214.
39. Martens, W. N.; Frost, R.L., Williams, P. Raman and infrared spectroscopic study of the basic copper chloride minerals: implications for the study of the copper and brass corrosion and "bronze disease". *Neues Jahrbuch für Mineralogie. Abhandlungen* 2003, 178(2):197-215.
40. Frost, R.L.; Yang, J.; Ding, Z. Raman and FTIR spectroscopy of natural oxalates: Implications for the evidence of life on Mars. *Chin.Sci.Bull*, 2003, 48, 1844–1852.
41. Van der Weerd, J.; Van Loon, A.; Boon, J.J. FTIR studies of the effects of pigments on the aging of oil. *Stud Conserv*, 2005, 50:3–22.
42. Vetter, W.; Latini, I.; Schreiner, M. Azurite in medieval illuminated manuscripts: a reflection-FTIR study concerning the characterization of binding media. *Herit Sci*, 2019, 7:21.
43. Filopoulou, A.; Vlachou, S.; Boyatzis, S.C. Fatty Acids and Their Metal Salts: A Review of Their Infrared Spectra in Light of Their Presence in Cultural Heritage. *Molecules*, 2021, 26, 6005.
44. Robinet, L.; Corbeil, M.C. The characterization of metal soaps. *Stud Conserv*, 2003, 48:23–40.
45. Otero, V.; Sanches, D.; Montagner, C.; Vilarigues, M.; Carlyle, L.; Lopes, J.A.; Melo, M.J. Characterisation of metal carboxylates by Raman and infrared spectroscopy in works of art. *J Raman Spectrosc*, 2014, 45:1197–1206.
46. Pellegrini, D.; Duce, C.; Bonaduce, I.; Biagi, S.; Ghezzi, L.; Colombini, M.P.; Tinè, M.R.; Bramanti, E. Fourier transform infrared spectroscopic study of rabbit glue/inorganic pigments mixtures in fresh and aged reference paint reconstructions, *Microchemical Journal*, 2016, 124: 31-35.
47. Guglielmi, V.; Andreoli, M.; Comite, V.; Baroni, A.; Fermo, P. The combined use of SEM-EDX, Raman, ATR-FTIR and visible reflectance techniques for the characterisation of Roman wall painting pigments from Monte d’Oro area (Rome): an insight into red, yellow and pink shades. *Environ Sci Pollut Res* 2022, 29, 29419–29437.
48. Müller, C.; Pejcic, B.; Esteban, L.; Delle Piane, C.; Raven, M.; Mizaikoff, B. Infrared Attenuated Total Reflectance Spectroscopy: An Innovative Strategy for Analyzing Mineral Components in Energy Relevant Systems. *Sci Rep*, 2014, 4:6764.
49. Ellerbrock, R.; Stein, M.; Schaller, J. Comparing amorphous silica, short-range-ordered silicates and silicic acid species by FTIR. *Sci Rep*, 2022, 12:11708.